



# Organic–inorganic nanocomposites for shape memory effects

High Performance Polymers  
23(7) 518–525

© The Author(s) 2011

Reprints and permission:

sagepub.co.uk/journalsPermissions.nav

DOI: 10.1177/0954008311424319

hip.sagepub.com



Cha Young Bae<sup>1</sup>, Hong Chae Park<sup>2</sup> and Byung Kyu Kim<sup>1</sup>

## Abstract

Polyurethane (PU)–silica nanocomposites were synthesized by sol–gel reactions between the surface silanol groups of fumed silica and 3-aminopropyltriethoxysilane (APTES) terminated PU with a broad range of silica contents (1–5%) with two different molecular weights of PU. It was found that the silica particles that were incorporated into the polymer chains were well dispersed in the PU matrix and acted as multifunctional cross-links and reinforcing fillers; in addition, the silica particles augmented the initial and rubbery moduli, yield, and break strengths, as well as the glass transition temperature. Moreover, 98–99% shape fixity and shape recovery with minimum cyclic hysteresis were obtained with only 1% silica particle loading.

## Keywords

Shape memory polyurethane, nanocomposites, sol–gel reaction

## Introduction

Shape memory polymers (SMPs) respond to external stimuli such as heat, electrical fields, and magnetic fields, and they are steadily expanding their usages in coatings, adhesives, sportswear, and textiles, as well as in traditional packaging materials.<sup>1,2</sup> Furthermore, ample potential applications are opening in new areas, like biomedical devices and space materials, with the enhancement of the mechanical performance and multiple functionalizations of SMPs. Excellent reviews have become available along with the recent developments.<sup>3–6</sup>

A comprehensive review regarding SMP composite has recently become available.<sup>3</sup> Mechanical reinforcements and functionalizations are largely achieved by physical and chemical hybridizations of SMPs with fillers in the forms of particles, fibers, platelets, or tubes. Generally, chemical incorporation on the nano-scale is superior to the physical blending on the macro-scale due to the fine dispersion and improved interfaces between the SMPs and fillers. However, the results suggest partial successes.

Chemical incorporation of crystalline polyhedral oligomeric silsesquioxane (POSS) nanoparticles as the hard segment in SM polyurethane (PU) exhibited over 99% shape fixity but poor shape recovery (71%) for the first cycle.<sup>7</sup> Physical and chemical incorporations of layered nanoclay augmented the mechanical strength

of SMPU but decreased the shape recovery.<sup>8–10</sup> However, when the silica nano-particles are chemically incorporated into the amorphous SMPU as multifunctional cross-links, over 99% shape fixity and shape recovery with minimum cyclic hysteresis were obtained.<sup>11,12</sup>

In the present study, a broad range of silica particles (1–5%) were chemically incorporated into the PU as multifunctional chemical cross-links or chain extenders. PU is a most versatile material to control the shape memory properties.<sup>13,14</sup> The PU was end capped with 3-aminopropyltriethoxysilane (APTES) to make sol–gel reactions with the silanol groups on the particle surfaces.

So the molecular weight of the PU ( $M_{PU}$ ) becomes the molecular weight between the cross-links ( $M_C$ ), which are the fumed silica particles. Shape memory performance as well as mechanical, dynamic-mechanical, and surface properties of

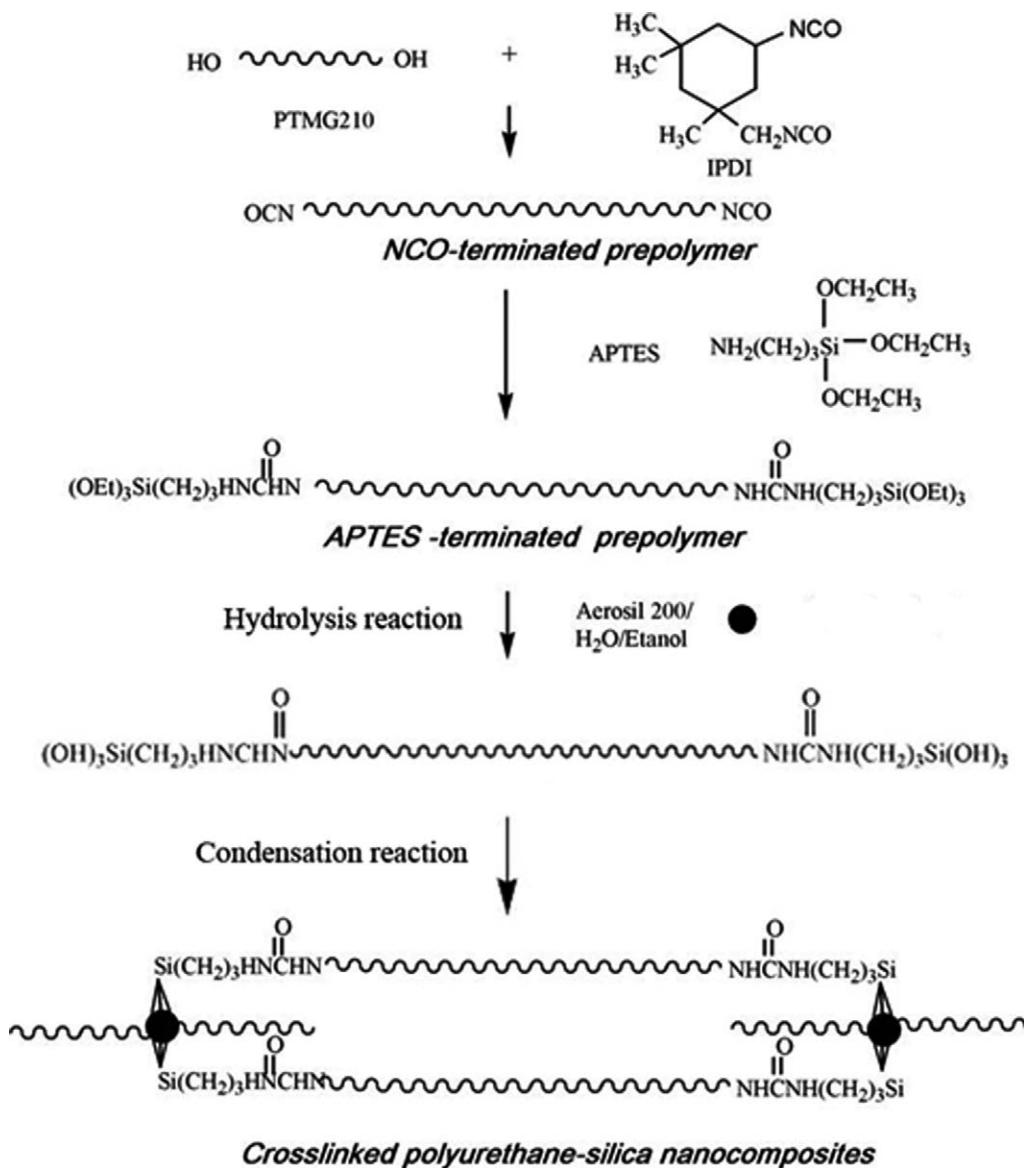
<sup>1</sup>Department of Polymer Science and Engineering, Pusan National University, Busan, Korea

<sup>2</sup>School of Materials Science and Engineering, Pusan National University, Busan, Korea

## Corresponding Author:

Byung Kyu Kim, Department of Polymer Science and Engineering, Pusan National University, Busan 609-735, Korea

Email: bkkim@pnu.edu



**Scheme 1.** Overall reaction scheme for preparing the polyurethane-silica nanocomposites.

the chemical hybrids were measured according to the amount of silica and  $M_{\text{PU}}$ .

## Experimental

### Materials

Poly(tetramethylene glycol) (PTMG;  $M_n = 210$ ) (KPX, Korea) was dried and degassed at 80 °C under vacuum for 3 h. Isophorone diisocyanate (IPDI; Aldrich), dibutyltin dilaurate (DBTDL; Aldrich), and 3-aminopropyltriethoxysilane (APTES; Aldrich) were used as received. Hydrophilic silica (fumed silica, Aerosil 200) with an average primary size of 12 nm and an aggregate size of about 100 nm was obtained from Evonik.

### Preparation of polyurethane nanocomposites

The overall reaction scheme for the synthesis of the composite is shown in Scheme 1. PTMG was first reacted with IPDI in dimethyl formamide (DMF) at 60 °C for 4 h using a four-necked separable flask equipped with a mechanical stirrer, a thermometer, a condenser, and a nitrogen injection tube. This reaction yielded NCO-terminated prepolymers with theoretical molecular weights of 3000 and 7000 ( $M_{\text{PU}}$ ), as determined by the  $[\text{NCO}]/[\text{OH}]$  index. These prepolymers were end-capped with APTES at 60 °C for 3 h. Finally, the silica particles dispersed in DMF were fed into the solutions at various compositions, as given in Table 1. To improve the dispersion of silica particles in DMF, silica was added to DMF in a vial and was ultrasonicated for 60 min before the mixture was added to the polymer

**Table 1.** Formulations to synthesize shape memory polyurethane-silica nanocomposites and contact angle of the film with water drops.

	PTMG210 (mol)	IPDI (mol)	APTES (mol)	Silica (%)	$M_c$ ( $\text{g mol}^{-1}$ )	Contact angle ( $^\circ$ )	$N$ ( $\times 10^{33} \text{ m}^{-3}$ )
P30	5.40	6.40	2	0	3000	72	4.81
P70				0		70	6.09
P71	14.65	15.65	2	1	7000	78	7.50
P73				3		87	9.11
P75				5		91	9.89

$N$  is the number density of faussian chains.

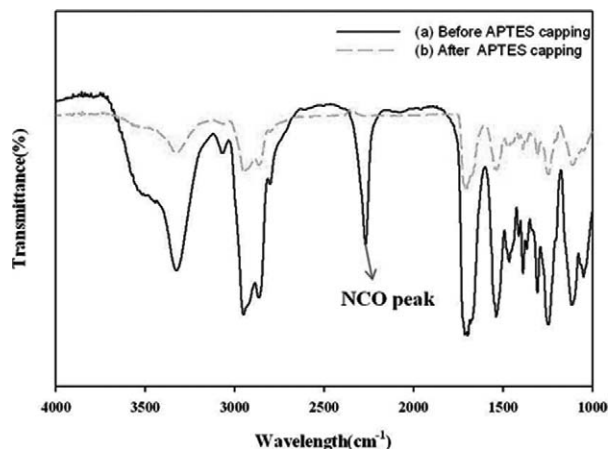


**Figure 1.** FTIR spectra of the polyurethane before (a) and after (b) APTES capping.

solution. To hydrolyze the ethoxy groups of the APTES, a 1 : 1 mixture of distilled water and ethanol (0.2%) was added to the prepolymer solution. Subsequently, the polymer solutions were cast on a Teflon plate and dried to form films. To completely remove the DMF, film was dried at 80 °C for 3 days, followed by drying in a vacuum oven at 50 °C for the next 3 days until the weight of film becomes constant. The condensation reactions between the silanol groups of APTES and the silica surface occurred during drying in an oven at 80 °C, resulting in the cross-links between the polyurethane and silica particles.

### Measurements

Fourier transform infrared (FTIR) spectroscopy was used to confirm the end capping of the NCO terminal with APTES. FTIR was also used to confirm the sol-gel reactions between the APTES and the Si-OH groups on the surface of the silica particles.

The tensile properties of the cast films were measured at room temperature with a universal testing machine (UTM; Lloyd LRX) at a crosshead speed of 500 mm min<sup>-1</sup> using specimens prepared according to ASTM D-1822. Dynamic-mechanical tests were performed

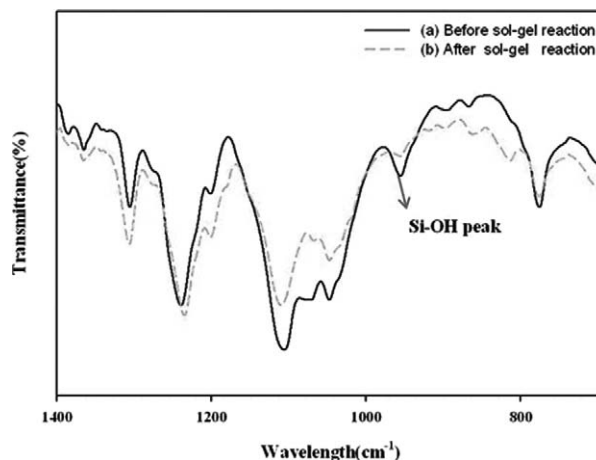


**Figure 2.** FTIR spectra of the virgin silica (a) and the silica after reaction with APTES (b).

using a dynamic-mechanical thermal analyzer (DMTA) (Rheometrics, MK-IV) at 10 Hz, 5 °C min<sup>-1</sup>, and 2% strain from -20 to 150 °C.

The morphology of the film was examined under scanning electron microscopy (SEM; Hitachi S430). Films were fractured in liquid nitrogen and the fractured structures were scanned.

The contact angles of the dispersion cast films with deionized water were measured with a conventional contact angle goniometer (G-1; Erma). The tests were performed at room temperature and the results reported are the average values of at least five runs.

The shape memory properties were characterized using an UTM (Lloyd LRX) attached with a heating chamber.

The sample was first heated to a loading temperature of  $T_g + 20$  °C and loaded to a maximum strain ( $\epsilon_m$ ) of 100% at a crosshead speed of 200 mm min<sup>-1</sup>, followed by cooling and unloading at  $T_g - 20$  °C. Upon unloading, part of the strain ( $\epsilon_m - \epsilon_u$ ) was instantaneously recovered, leaving an unload strain ( $\epsilon_u$ ). Then, the sample was reheated to the loading temperature of  $T_g + 20$  °C to recover the strain, leaving a substantial amount of permanent strain ( $\epsilon_p$ ). These three steps complete one thermomechanical cycle. Shape fixity and shape recovery are defined as:

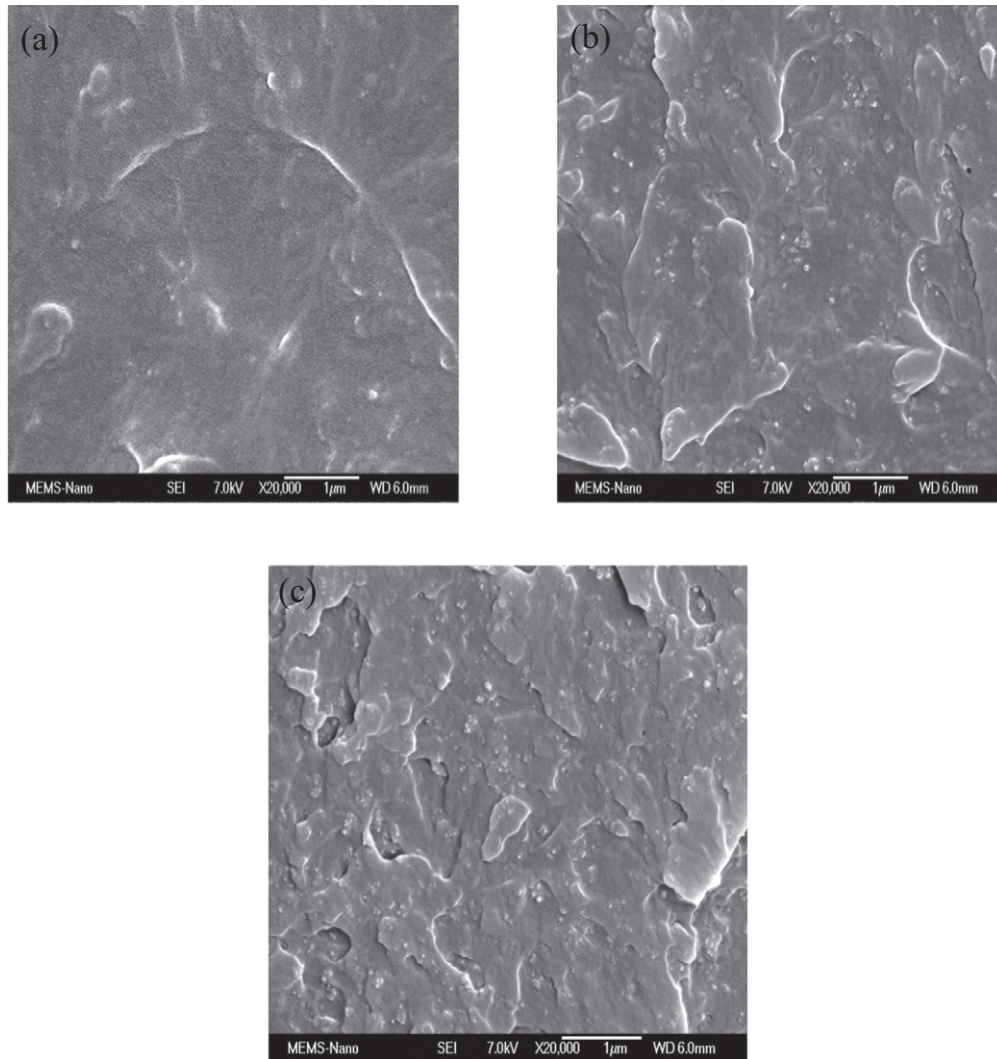


**Figure 3.** SEM images of the polyurethane-silica nanocomposite: 1% (a); 3% (b); and 5% (c) silica.

$$\% \text{ shape fixity} = \frac{\varepsilon_u}{\varepsilon_m} \times 100$$

$$\% \text{ shape recovery} = \frac{\varepsilon_r}{\varepsilon_m} \times 100$$

where  $\varepsilon_r = \varepsilon_m - \varepsilon_p$  is the recovered strain.

## Results and discussion

### Confirmation of APTES capping by FTIR spectroscopy

The FTIR spectra of the NCO-terminated PU prepolymer and APTES capped prepolymer are given in Figure 1, which shows that the absorption peak at about  $2270 \text{ cm}^{-1}$

- (1) corresponding to the stretch vibration of the NCO group has completely disappeared upon capping with APTES.

(2) **Confirmation of sol-gel reaction by FTIR spectroscopy**

The FTIR spectra of the virgin silica and the silica after reaction with APTES are shown in Figure 2 where the absorption band at  $955 \text{ cm}^{-1}$ , which was assigned to the stretching of the terminal Si-OH of the silica, almost disappeared after the sol-gel reactions.

### SEM image

The SEM images of the nanocomposites are shown in Figure 3. Neither aggregates nor agglomerates of the silica particles were seen at the high particle concentration (5%).

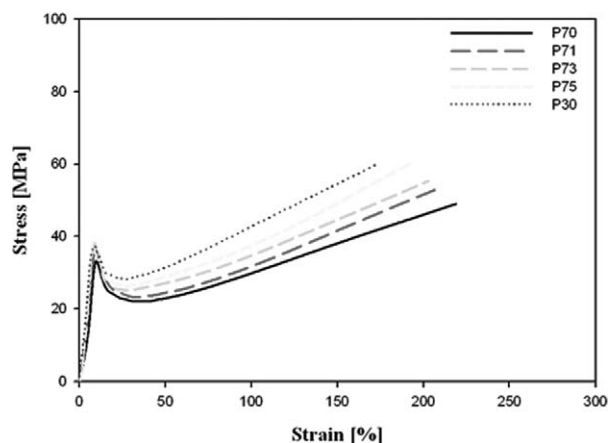


**Figure 4.** Stress–strain behaviour of the polyurethane–silica nanocomposites at 25 °C.

The particles are well dispersed in the polymer matrix by incorporating the particles via covalent bonds.

### Contact angles

Although minor, the surface properties of SM film are important for certain areas, such as dental and automobile applications. The contact angle of the film with water drops was greater with P30 than with P70 and increased with the increase in silica content (Table 1). The contact angle is expected to decrease with the increase of hydrophilic silica particles. The present result is in contradiction to this. The present results are based on the increased geometrical area relative to the projection area due to the increased surface area with silica inclusion.<sup>15</sup> This can be visualized by atomic force microscopy.<sup>12</sup>

### Mechanical properties

The stress–strain behavior of the nanocomposites at 25 °C is shown in Figure 4. Both types of PU (P30, P70) cross-linked by APTES show positive yield, necking, and strain hardening. However, these values were greater with P30 than with P70 due to the high cross-link density of P30, namely, due to the smaller  $M_{PU}$ .

With the addition and increasing amount of silica particles, the modulus, yield, and break strength monotonically increased and elongation at break decreased. The monotonic increase is expected from the fine dispersion of silica particles, even at high concentrations. This led to the increased area under the curve, which is important in SMP since the area is strain energy stored during stretching and it drives strain recovery upon release of stress in its rubbery state. The results are based on the dual effects of silica nanoparticles as multifunctional chemical cross-links and reinforcing fillers.<sup>11</sup>

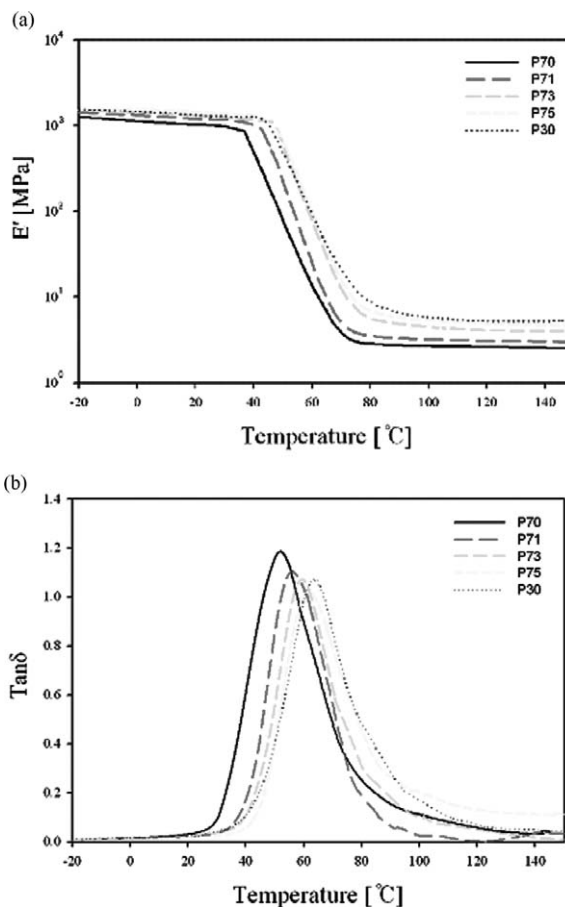


**Figure 5.** Storage modulus (a) and  $\tan \delta$  (b) of the polyurethane silica nanocomposites plotted against temperature.

Multifunctional cross-links provide the hybrid materials with high cross-link density while fillers augment the rigidity of the material.

### Dynamic mechanical properties

Figure 5 shows the dynamic mechanical properties of the polyurethane nanocomposites. All the samples have well-defined rubbery plateaus, indicative of the cross-linked structure. In addition, all the samples have relatively narrow glass to rubber transitions and about three orders of magnitude difference in glass and rubbery state moduli. Both properties are highly desirable for shape memory applications.<sup>5</sup> A narrow transition results in high-temperature sensitivity while a high modulus ratio results in high shape fixity. The narrow transition is due to the intensive phase mixing between the soft and the hard segments, which was achieved by incorporating relatively low-molecular-weight polyols.<sup>16,17</sup>

The rubbery modulus ( $G_N$ ) and the  $\tan \delta$  peak temperature corresponding to the glass transition temperature ( $T_g$ ) increase with the addition and increasing amount of silica particles. The role of silica particles is dual; it acts as both a filler

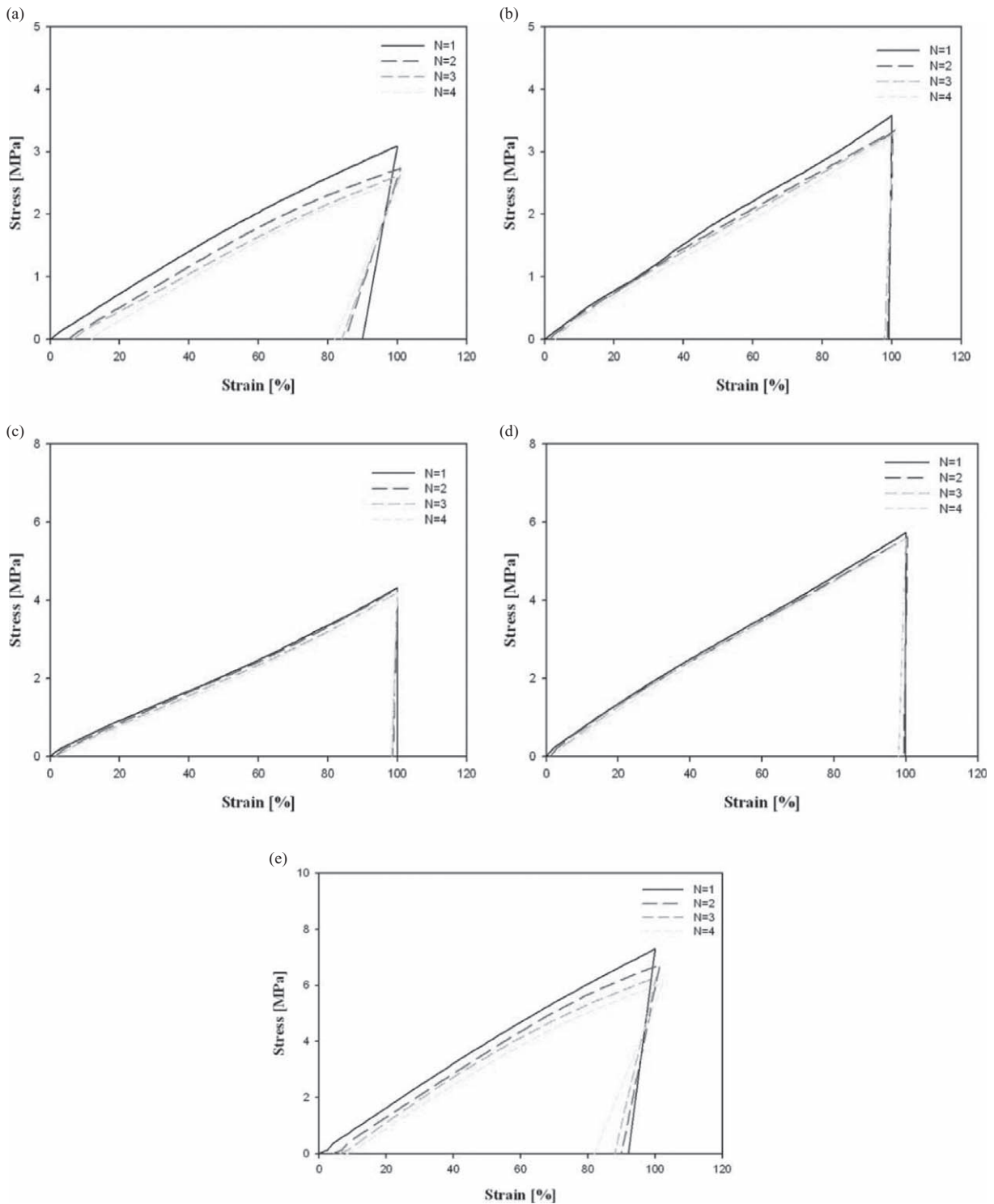


**Figure 6.** Thermomechanical cyclic behavior: P70 (a); P71 (b); P73 (c); P75 (d); and P30 (e)

and multifunctional cross-link. As a filler, silica particles augment the rigidity and retard the segmental motion of the polymer chains. As a cross-link, the silica's function can be described by the ideal rubber theory where the plateau modulus is given by the following equation:<sup>18</sup>

$$G_N^0 = \frac{\rho RT}{M_C} = NkT,$$

where  $\rho$  is the density,  $T$  is the absolute temperature,  $R$  is the gas constant,  $k$  is the Boltzmann constant, and  $N$  is the

**Table 2.** Shape memory properties of polyurethane-silica nanocomposites.

	Shape fixity(%)					Shape recovery(%)				
	P30	P70	P71	P73	P75	P30	P70	P71	P73	P75
$N = 1$	92	90	98	99	99	96	95	98	99	98
$N = 2$	90	85	98	98	98	94	94	98	99	98
$N = 3$	88	84	98	98	98	92	89	97	98	98
$N = 4$	82	82	97	98	98	89	87	97	98	98

$N$ , number of thermomechanical cycles.

number density of the polyurethane sub-chains which increases linearly with the functionality of the cross-link. The calculated values of  $N$  are shown in Table 1. It is also noted that 3000  $M_C$  yields a higher rubbery modulus and  $T_g$  than 7000  $M_C$ , which is in agreement with the above equation. The amount of chemically incorporated silica particles and  $M_{PU}$  are useful parameters for controlling the elastic properties of the nanocomposites.

### Shape memory behavior

The typical cyclic loading and unloading behavior of the PU hybrids operating at 80–10–80 °C (deformed-frozen-recovered) are shown in Figure 6 for the first four cycles and the detailed data are given in Table 2. The films are in rubbery state at 80 °C and glassy state at 10 °C. The shape fixity and shape recovery of the unfilled films were a bit greater with P30 (92, 96%) than P70 (90, 95%) and decreased as the number of cycles increases from one to four. The effect of the silica was studied with the P30 series. The shape fixity and shape recovery increased to 98% with the incorporation of 1% silica and the value is essentially not changed with further additions. Moreover, these properties are mostly retained during the four thermo-mechanical cycles. This results in a significant improvement in hysteresis resistance over the unfilled film due to the triple effect of silica particles as multifunctional cross-linker, reinforcing filler, and stress relaxation retarder.<sup>19</sup> The hysteresis resistance is of importance since SMPs are often subject to repeated loadings and unloadings.<sup>1</sup>

### Conclusions

Shape memory polyurethane-silica nanocomposites were synthesized by sol-gel reactions between the surface silanol groups of fumed silica and hydrolyzed APTES-terminated PU prepolymers with a broad range of silica contents. It was shown that the silica particles incorporated into the polymer chains were well dispersed in the polymer matrix, and they acted as multifunctional cross-links as well as reinforcing fillers, and they augmented the initial and rubbery moduli, yield, and break strengths, as well as the glass transition temperature. Notably, 98–99% shape fixity and shape

recovery with minimum cyclic hysteresis were obtained with only 1% silica particle loading incorporated into the polyurethane chain.

### Acknowledgement

The research was supported by NCRC at PNU.

### References

- Behl M, Razzaq MY and Lendlein A. Multifunctional shape-memory polymers. *Adv Mater* 2010; **22**: 3388–3410.
- Kim BK. New frontiers of shape memory polymers. *Express Polym Lett* 2010; **4**: 589.
- Madbouly S and Lendlein A. Shape-memory polymer composites. *Adv Polym Sci* 2010; **226**: 41–95.
- Liu C, Qin H and Mather PT. Review of progress in shape-memory polymers. *J Matl Chem* 2007; **17**: 1543–1558.
- Ratna D and Karger-Kocsis J. Recent advances in shape memory polymers and composites: A review. *J Mater Sci* 2008; **43**: 254–269.
- Meng H and Hu J. A brief review of stimulus-active polymers responsive to thermal, light, magnetic, electric, and water/solvent stimuli. *J Intel Mater Syst Struct* 2010; **21**: 859–885.
- Knight PT, Lee KM, Qin H and Mather PT. Thermoplastic polyurethanes incorporating polyhedral oligosilsesquioxane (POSS). *Biomacromolecules* 2008; **9**: 2458–2467.
- Cao F and Jana SC. *Polymer* 2007; **48**: 3790–3800.
- Liang C, Rogres CA and Malafeev EJ. Nanoclay-tethered shape memory polyurethane nanocomposites. *J Intell Mater Syst Struct* 1997; **8**: 380–386.
- Ohki T, Ni Q, Ohako N and Iwamoto M. Mechanical and shape memory behavior of composites with shape memory polymer. *Composites A* 2004; **35**: 1065–1073.
- Jang MK, Hartwig A and Kim BK. Shape memory polyurethanes cross-linked by surface modified silica particles. *J Matl Chem* 2009; **19**: 1166–1172.
- Jung DH, Jeong HM and Kim BK. Organic-inorganic chemical hybrids having shape memory effect. *J Matl Chem* 2010; **20**: 3458–3466.
- Hong SJ, Yu WR and Youk JH. Two-way shape memory behavior of shape memory polyurethanes with a bias load. *Smart Mater Struct* 2010; **19**: 1–9.

14. Yang JH, Chun BC, Chung YC and Cho JH. Comparison of thermal/mechanical properties and shape memory effect of polyurethane block-copolymers with planar or bent shape of hard segment. *Polymer* 2003; **44**: 3251–3258.
15. Lafuma A and Quéré D. Superhydrophobic states. *Nat Mater* 2003; **2**: 457–460.
16. Kim BK, Lee SY and Xu M. Polyurethane having shape memory effects. *Polymer* 1996; **37**: 5781–5793.
17. Lee SH, Kim JW and Kim BK. Shape memory polyurethanes having crosslinks in soft and hard segments. *Smart Mater Struct* 2004; **13**: 1345–1350.
18. Gedde UW. *Polymer Physics*. London: Kluwer Academic Publishers, 1999.
19. Lee SK, Yoon SH, Chung I, Hartwig A and Kim BK. Waterborne polyurethane nanocomposites having shape memory effects. *J Polymer Sci Polymer Chem* 2011; **49**: 634–641.